Smoothed Particle Hydrodynamics Simulations for Asteroid Deflection

Maximilian Rutz

Abstract

Contents

1 Introduction

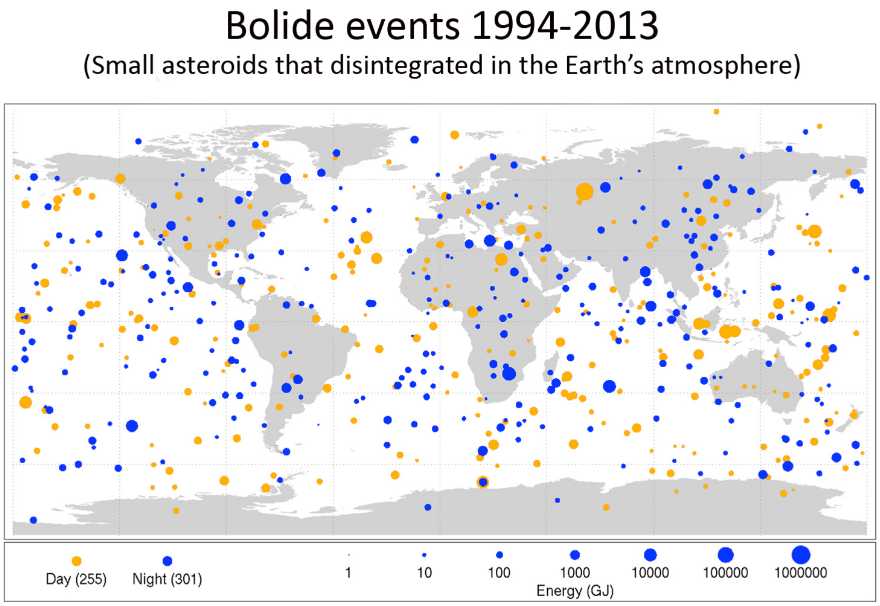

Figure 1: Past impacts [8]

- Dart and Hera Missions

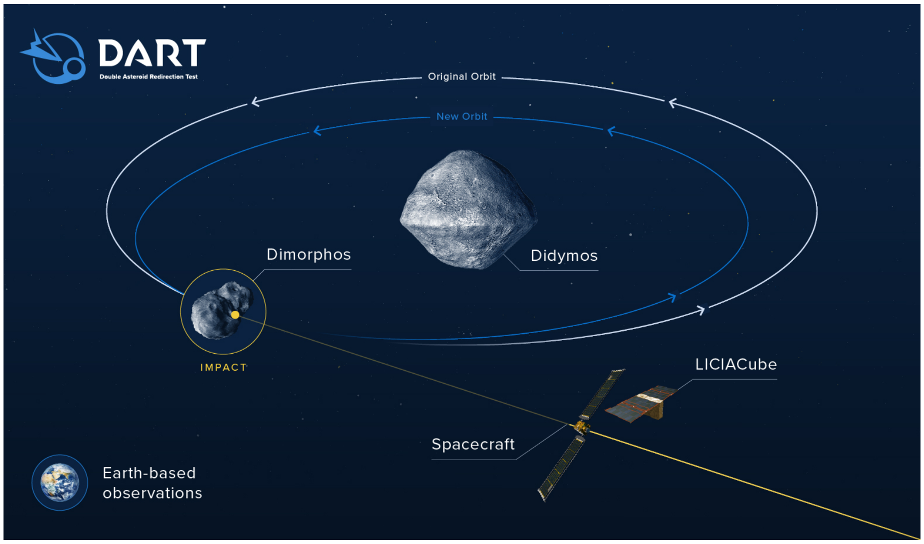

Figure 2: Dart mission [7]

Previous work: - Raducan [6] grid based 2d sims - Stickle [5] sph sims
Improvement of previous work: - Effect of impact angle on beta factor
Outline of the rest of the paper

2 Theory

2.1 Smoothed Particle Hydrodynamics

2.2 Main concept

Smoothed Particle Hydrodynamics is a numerical simulation method first introduced by [2] in 1977. It is a Lagrangian particle method and as such often used when the geometry of the underlying problem makes it difficult to apply Eulerian grid-based methods like finite difference schemes. Although SPH is most often used to model liquids, it is possible to add physical models for solids as well.

A SPH simulation is composed of many individual SPH particles. Each particle moves through space with a velocity $\vec{v}$ and a mass m. In contrast to particle methods used for N-body simulations or molecular dynamics, SPH particles carry information about continuous variables such as the density ρ or energy e. The particles only act as computational points at which equations from hydrodynamics/continuum mechanics such as the Euler or Navier-Stokes Equations are evaluated. Solving such equations comes down to converting partial differential equations to a system of first order ordinary differential equations in time.

$$\frac{d\vec{y}}{dt} = f(t, \vec{y}(t), A_1, ..., A_n) \tag{1}$$

In equation 1 $\vec{y}$ is a vector of quantities to be projected forward in time and A_1 through A_n are quantities that are calculated at every step. Once A_1 through A_n are known for every particle and the right hand side of quation 1 can be evaluated, standard integrators such as Runge-Kutta or Predictor-Corrector methods are used to update $\vec{y}$.

To calculate a quantity A at a particle location, SPH uses a weighted average of A over all particles in the neighborhood:

$$A(\vec{r}) \approx \int A(\vec{r}\,')W(\vec{r} - \vec{r}\,', h)\mathrm{d}\vec{r}\,' \tag{2}$$

The kernel function $W(|\vec{r} - \vec{r'}|$, h) at the particle location $\vec{r}$ depends upon the distance to the other particles and a specific length h called the smoothing length. Most kernels used today have compact support within a radius of h. To ensure normalization of the kernel

$$\int W(\vec{r} - \vec{r}\,', h)\mathrm{d}\vec{r}\,' = 1 \tag{3}$$

in the practial case of a finite number of particles, the density is added to

$$A_S(\vec{r}) = \lim_{h \to \infty} \int \frac{A(\vec{r}\,')}{\rho(\vec{r}\,')} W(\vec{r} - \vec{r}\,', h)\rho(\vec{r}\,')\mathrm{d}\vec{r}\,' \propto \sum_{b=1}^{N} m_b \frac{A_b}{\rho_b} W(\vec{r} - \vec{r}\,', h) = A_b \tag{4}$$

$$\int W(|\vec{r} - \vec{r'}|, h) dr' = 0 \tag{5}$$

Figure 3 illustrates

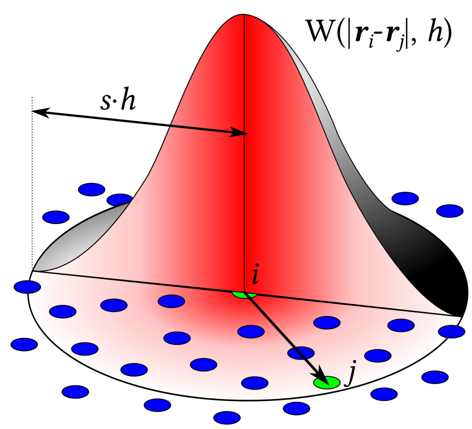

Figure 3: Kernel function [9]

2.2.1 Variable Smothing length

2.2.2 Artificial viscosity

2.3 Conservation laws

2.4 Constitutive equations

2.5 Equation of State

The Tillotson equation of state [1]

2.6 Porosity model

There are different ways in which porosity can be modeled depending on the pore size. Depending on the simulation, macro porosity with pore sizes above the resolution of the simulation can be accounted for in the initial conditions. This however becomes impossible for granular material with sub-resolution sized grains and pores.

Microporosity models porosity as an additional material property and can be applied independently of the resolution.

In these simulations, a microporosity p-α model as outlined in [3] is used. The distention $\alpha \in [1, \inf)$ relates the current density ρ to the solid density ρ_s which is reached if the material is fully compressed. For a non-porous material α equals one.

$$\alpha \equiv \frac{\rho_s}{\rho} \tag{6}$$

Often the porosity ϕ is used instead of the distention α. They relate by

$$\phi = 1 - \frac{1}{\alpha} \tag{7}$$

Quadratic crush curve

2.7 Strength model

2.8 Damage model for brittle material

3 Numerical Setup

3.1 Miluphcuda SPH code

Miluphcuda is a smoothed particle hydrodynamics code that has been developed over several years at the University of Tuebingen by Christoph Schaefer and others. Its general use is well documented in [4].

3.2 Initial conditions

- Target basalt halfsphere - Impactor aluminium sphere - resolution bound to variable smoothing length - Uniform macro structure but random micro structure to avoid - seagen [10] used to create initial conditions

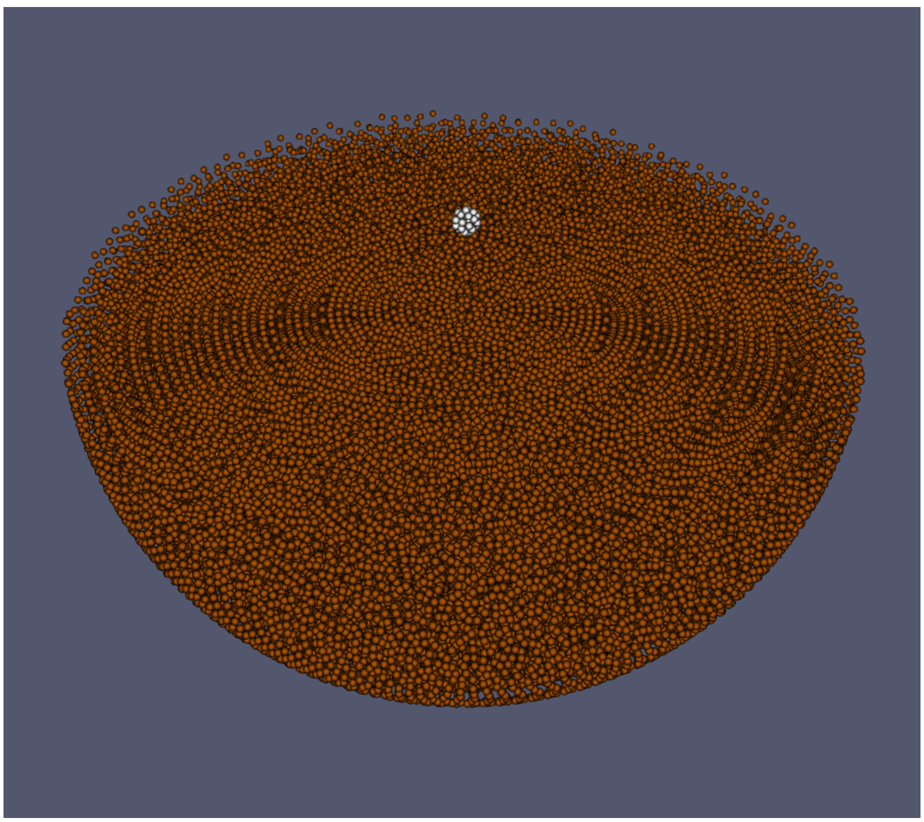

Figure 4: start of simulation

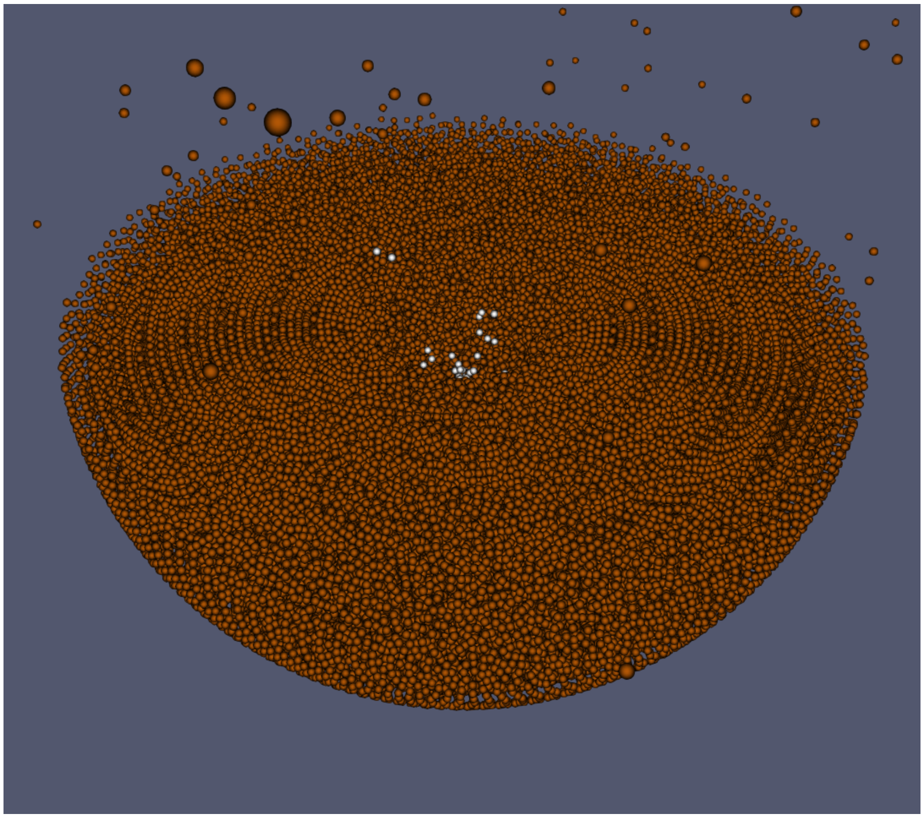

Figure 5: end of simulation

3.3 Material parameters

- variable smoothing length min 0.1 bis max 10.0 - rholimit 0.95

		Target	Projectile
Tillotson EOS	ρ_0	$2.86 \cdot 10^3 g \cdot cm^{-3}$	$2.70 \cdot 10^3 g \cdot cm^{-3}$
	A_T	$2.67 \cdot 10^{10}$ Pa	$7.52 \cdot 10^{10}$ Pa
	B_T	$2.67 \cdot 10^{10}$ Pa	$6.50 \cdot 10^{10}$ Pa
	E_0	$4.87 \cdot 10^8$ J	$5.00 \cdot 10^6$ J
	E_{iv}	$4.72 \cdot 10^6$ J	$3.00 \cdot 10^6$ J
	E_{cv}	$1.82 \cdot 10^7$ J	$1.39 \cdot 10^7$ J
	a_T	0.5	0.5
	b_T	1.5	1.63
	α_T	5.0	5.0
	β_T	5.0	5.0
Porosity	α_0	**varying**	not porous
	$p_{elastic}$	$1.0 \cdot 10^6$ Pa	not porous
	$p_{transition}$	$6.8 \cdot 10^7$ Pa	not porous
	$p_{compacted}$	$2.13 \cdot 10^8$ Pa	not porous
	α_e	4.64	not porous
	α_t	1.90	not porous
	c_s	$100.0\ m \cdot s^{-1}$	not porous
Strength	cohesive strength Y_c	**varying**	$1.0 \cdot 10^9$ Pa
	α	0.982793 rad	0 rad
	$\alpha_{damaged}$	0.540419 rad	0 rad
	shear modulus μ	$2.27 \cdot 10^{10}$ Pa	$2.69 \cdot 10^{10}$ Pa
	bulk modulus K_0	$2.67 \cdot 10^{10}$ Pa	$5.23 \cdot 10^{10}$ Pa
	yield stress Y_0	$3.5 \cdot 10^9$ Pa	$2.76 \cdot 10^8$ Pa
Weibull	M	16	no damage
	K	$1.0 \cdot 10^{61}$	no damage
Artificial viscosity	α	1.0	1.0
	β	2.0	2.0

Table 1: Material parameters for basalt target and aluminium Impactor

4 Results

The simulations were run with porosities of 0%, 17%, 33% and 50% and cohesive strengths of 1kPa, 10kPa, 100kPa and 1MPa under impact angles of 0 and 45 degrees. This yields 32 simulations in total.

4.1 Cratering

Figures 6 through 9 qualitatively show the effects of porosity and strength on the crater formation. The higher the porosity and the lower the porosity become, the wider and deeper the crater gets.

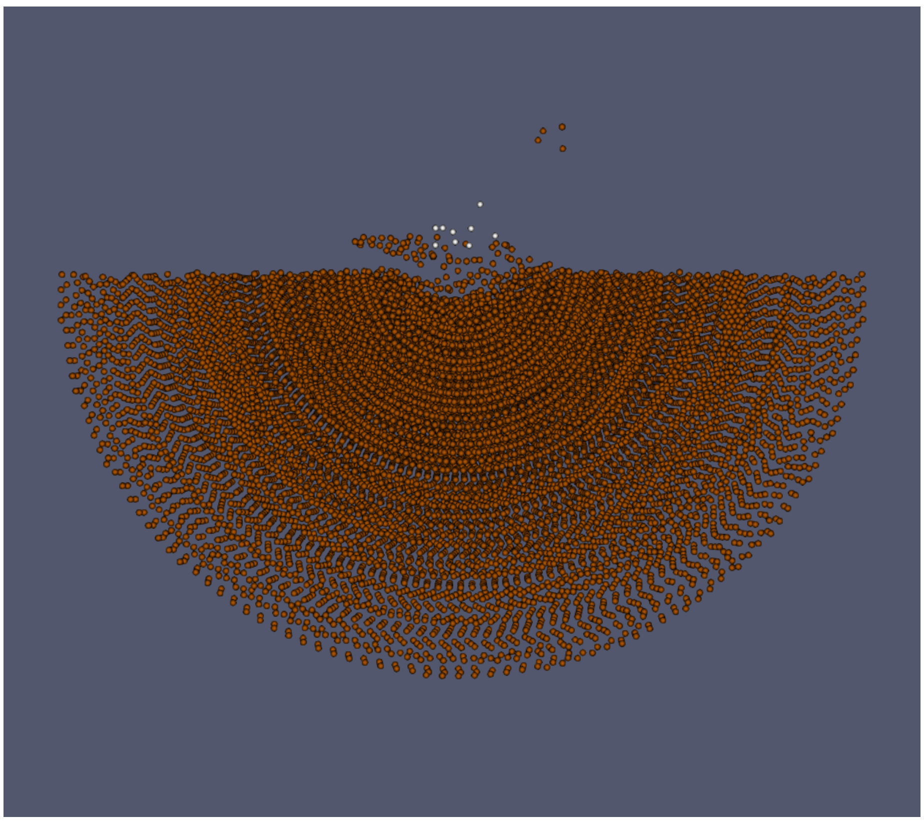

Figure 6: No porosity (0%), high strength (Y=1MPa)

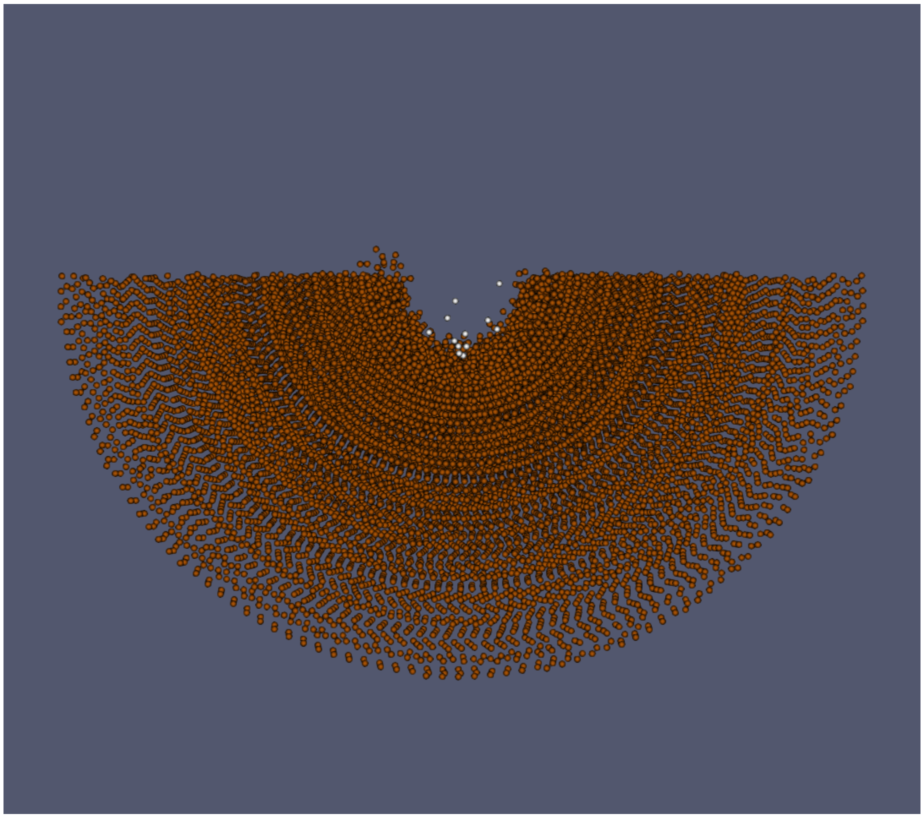

Figure 7: High porosity (50%), high strength (Y=1MPa)

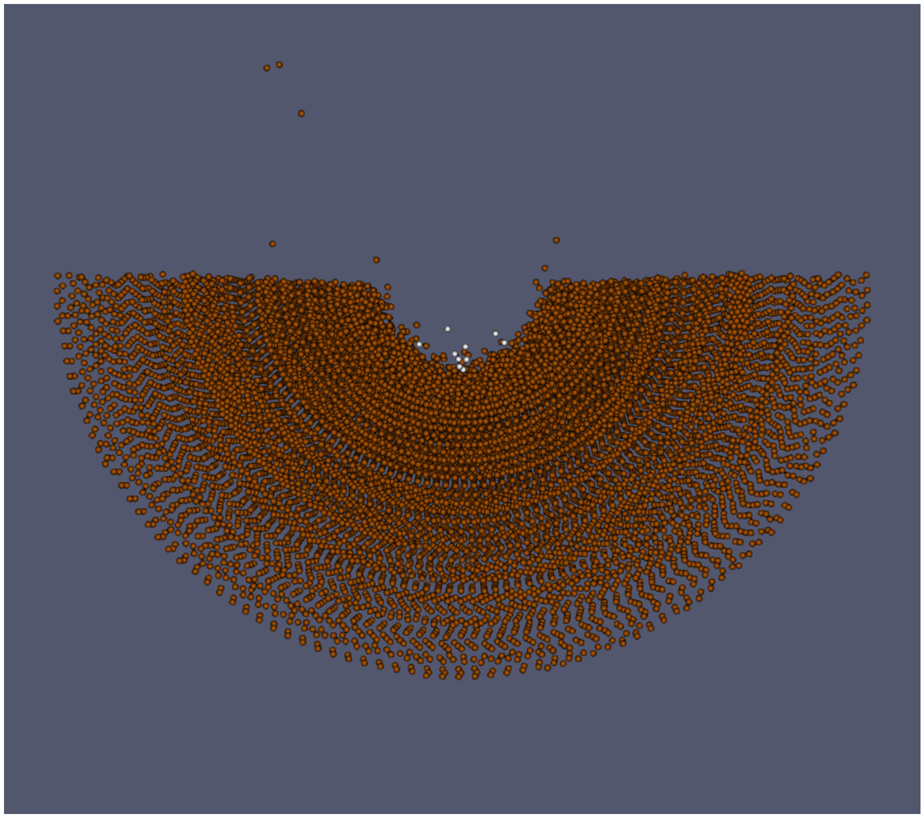

Figure 8: High porosity (50%), low strength (Y=1kPa)

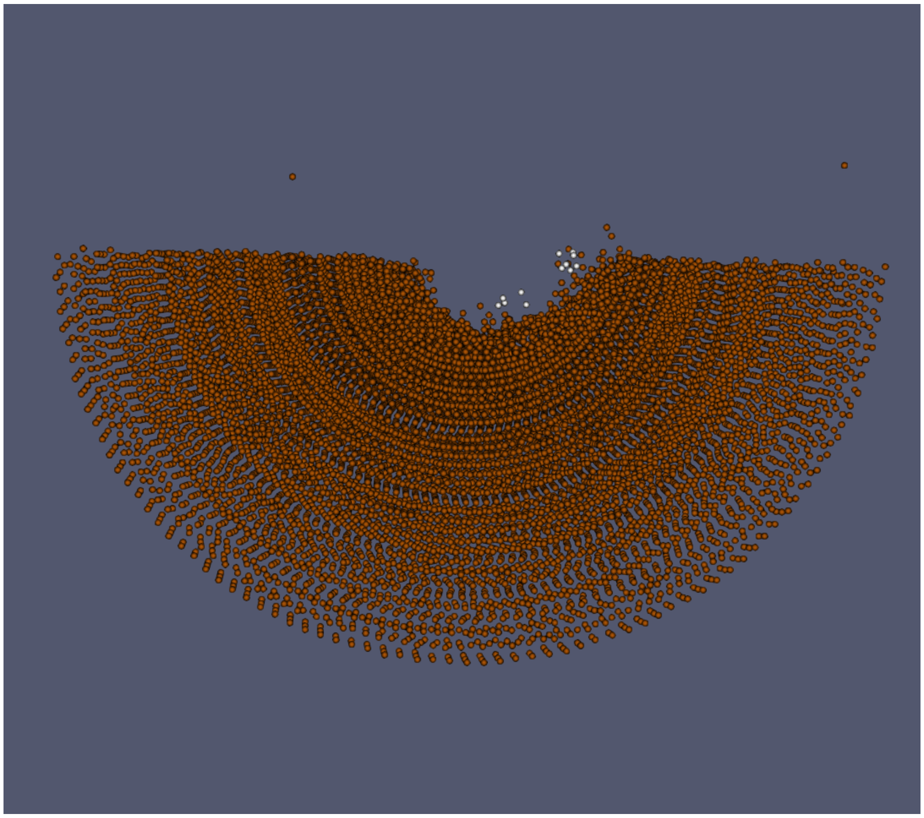

Figure 9: High porosity (50%), low strength (Y=1kPa), 45 degree angle

4.2 Beta factor

- explanation of beta factor

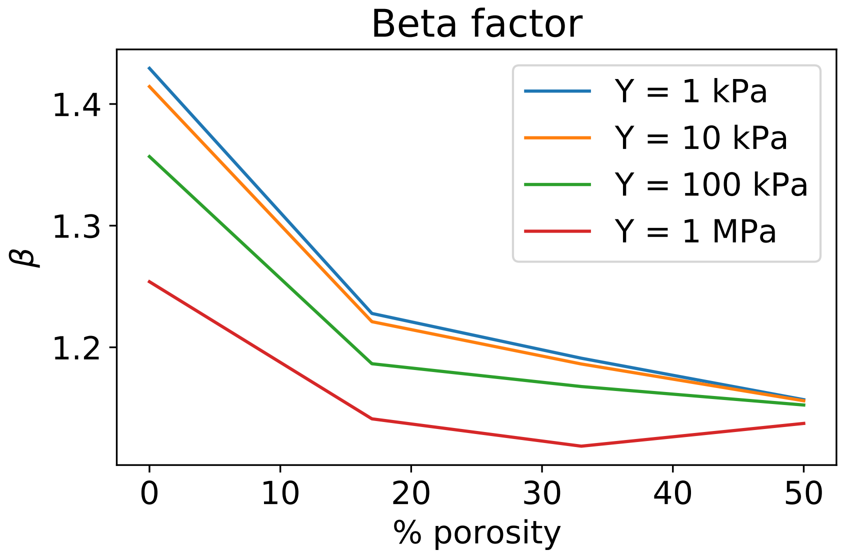

Figure 10: beta factor

5 Discussion

- beta factor lower than Raducan grid based but comparable to Stickle SPH - upper limit beta below 2 because of momentum conservation?? – which inertial system is used for calculation of beta factor in other papers? - tensorial correction not implemented because of timestep getting to small - no real boundary conditions implemented - the whole target shows shift (should not be a problem since we are still in the inertial frame of rest of the target !?)

References

[1] J. H. Tillotson. “Metallic Equations of State For Hypervelocity Impact”. In: (July 1962), p. 3216.

[2] R. A. Gingold and J. J. Monaghan. “Smoothed particle hydrodynamics: theory and application to non-spherical stars”. In: *Monthly Notices of the Royal Astronomical Society* 181.3 (Dec. 1977), pp. 375–389. ISSN: 0035-8711. DOI: 10.1093/mnras/181.3.375. eprint: https://academic.oup.com/mnras/article-pdf/181/3/375/3104055/mnras181-0375.pdf. URL: https://doi.org/10.1093/mnras/181.3.375.

[3] Martin Jutzi, Willy Benz, and Patrick Michel. “Numerical simulations of impacts involving porous bodies”. In: *Icarus* 198.1 (Nov. 2008), pp. 242–255. ISSN: 0019-1035. DOI: 10.1016/j.icarus.2008.06.013. URL: http://dx.doi.org/10.1016/j.icarus.2008.06.013.

[4] C. Schaefer et al. “A smooth particle hydrodynamics code to model collisions between solid, self-gravitating objects”. In: *Astronomy and Astrophysics* 590 (Apr. 2016), A19. ISSN: 1432-0746. DOI: 10.1051/0004-6361/201528060. URL: http://dx.doi.org/10.1051/0004-6361/201528060.

[5] A.M. Stickle et al. “Modeling impact outcomes for the Double Asteroid Redirection Test (DART) mission”. In: *Procedia Engineering* 204 (2017). 14th Hypervelocity Impact Symposium 2017, HVIS2017, 24-28 April 2017, Canterbury, Kent, UK, pp. 116–123. ISSN: 1877-7058. DOI: https://doi.org/10.1016/j.proeng.2017.09.763. URL: http://www.sciencedirect.com/science/article/pii/S1877705817343217.

[6] Sabina Raducan et al. “The role of asteroid strength, porosity and internal friction in impact momentum transfer”. In: *Icarus* 329 (Apr. 2019), pp. 282–295. DOI: 10.1016/j.icarus.2019.03.040.

[7] NASA/Johns Hopkins APL. [Online; accessed 22-September-2020]. 2020. URL: https://dart.jhuapl.edu/Gallery/media/graphics/lg/DART-infographic_v4.jpg.

[8] Wikimedia Commons. *File:SmallAsteroidImpacts-Frequency-Bolide-20141114.jpg — Wikimedia Commons, the free media repository.* [Online; accessed 20-September-2020]. 2020. URL: https://commons.wikimedia.org/w/index.php?title=File:SmallAsteroidImpacts-Frequency-Bolide-20141114.jpg&oldid=447357435.

[9] Wikimedia Commons. *File:SPHInterpolationColorsVerbose.svg — Wikimedia Commons, the free media repository.* [Online; accessed 20-September-2020]. 2020. URL: https://commons.wikimedia.org/w/index.php?title=File:SPHInterpolationColorsVerbose.svg&oldid=446219914.

[10] Jacob Kegerreis. *SEAGen.* https://github.com/jkeger/seagen. 2020.